

Biology I: Structural Biology and Macromolecular Crystallography (MX)

Thomas R. Schneider, EMBL Hamburg
26/6/2014
thomas.schneider@embl-hamburg.de



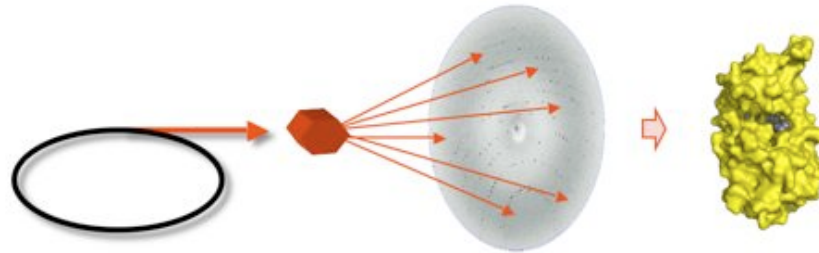
EMBL

- Funded 1974
- Inter-governmental organization
- 21 member states (+ Czech Rep)
- Two associate states (+Argentina)
- Missions
 - Basic Research in Molecular Biology
 - Technology and Instrumentation
 - Facilities and Services
 - Teaching and Training
 - Technology Transfer
- 5 sites
- 1400 employees from 60 nations
- Annual Budget ca. 85 M€



Biology I to IV

- Structural Biology and Macromolecular Crystallography (MX)
- MX - The method
- MX - Collection and processing of diffraction data
- MX - Building models and the future



Today

- What is a protein?
- The central dogma of molecular biology
- Milestones in macromolecular crystallography
 - The first structures
 - Recombinant production of proteins
 - Use of synchrotron radiation
 - Detector technologies
 - The protein data bank
 - Cryogenic sample cooling
- Crystallographic Workflow

Look at Abl kinase

- 2148 atoms per molecule, 275 amino acids
 - A protein consists of chained amino acids (20 types)
 - Backbone vs. Sidechain
 - alpha-helices
 - beta-sheets
 - Schematic 'cartoon' representations of proteins
 - Surface representation of proteins (with properties mapped)
 - Interactions with ligands can be studied
 - Gleevec / Imantinib
-
- Folding (Stretch out 275 amino acids -> $3.8 \text{ cm} \times 275 = 10.41 \text{ m}$, compare to $53 \text{ \AA} / \text{cm}$)

Downloads:

[molecule viewer](http://pymol.org/educational/): <http://pymol.org/educational/>

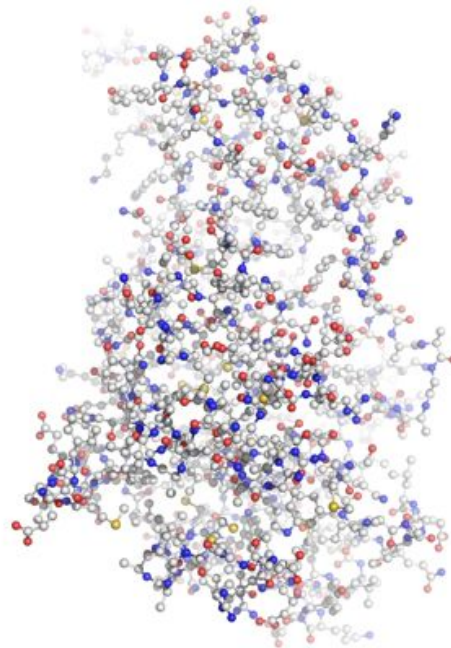
[pdb-model](http://www.rcsb.org/pdb/explore/explore.do?structureId=1FPU): <http://www.rcsb.org/pdb/explore/explore.do?structureId=1FPU>

[viewer script](#): see course website



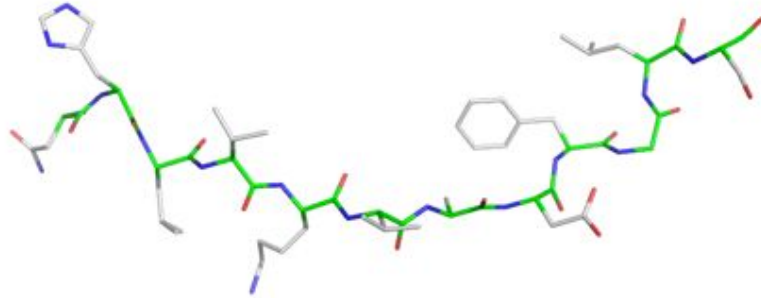
A protein molecule

- Looking at a collection of >2000 atoms can be rather confusing:



Polypeptide chain

- Proteins are heteropolymers of amino-acids:



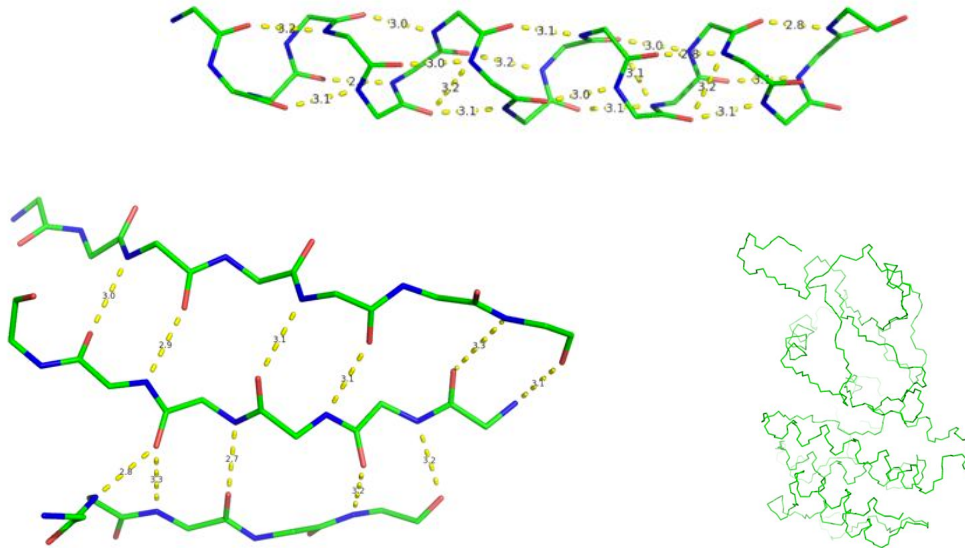
Protein Backbone

- Looking at the backbone only allows to follow the polypeptide chain across the protein



Protein conformation

- alpha helices and beta sheets contain repeating pattern / hydrogen bonds:

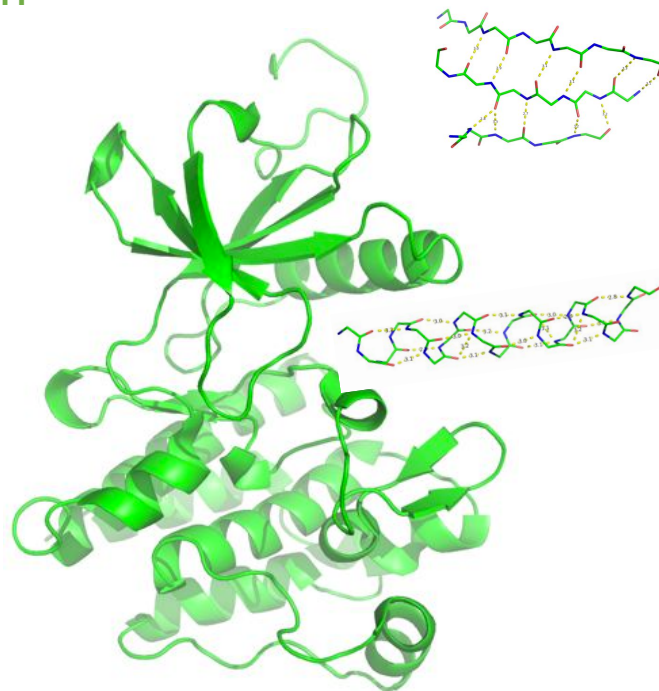


Thomas R. Schneider | Meth. moderner Röntgenphysik II | 25/6/2014 EMBL



Protein conformation

- Schematic representation of helices and sheets illustrates the 'fold'

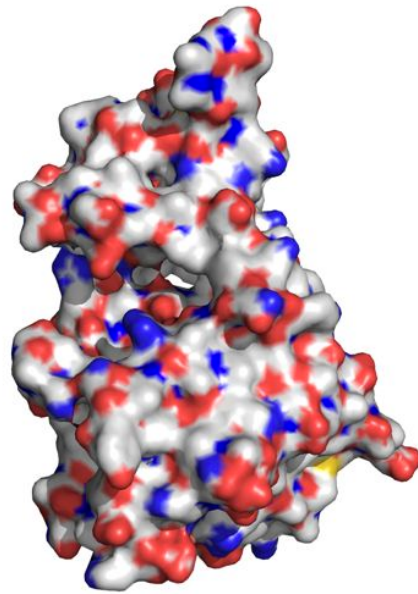


Thomas R. Schneider | Meth. moderner Röntgenphysik II | 25/6/2014 EMBL



Protein surfaces

- What other molecules 'see' is a molecular surface.
- Active sites are often found in cavities

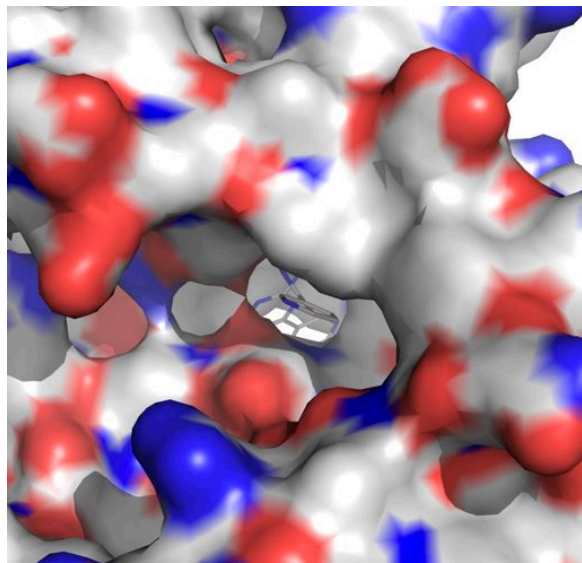


Thomas R. Schneider | Meth. moderner Röntgenphysik II | 25/6/2014



Active sites

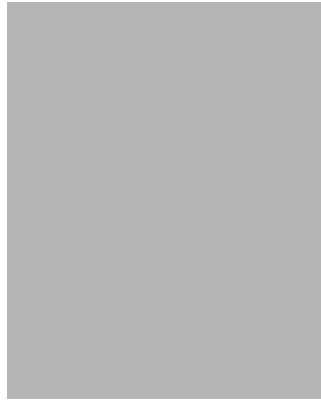
- Knowledge of the active site geometry allows to design ligands binding to the active sites thus acting as drugs.
- Here: Gleevec binding Abl-Kinase



Thomas R. Schneider | Meth. moderner Röntgenphysik II | 25/6/2014

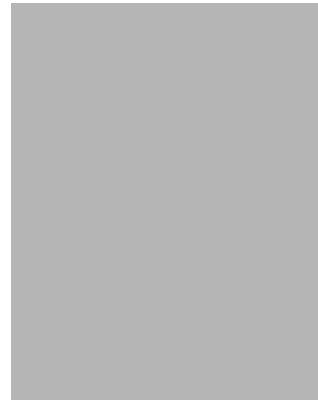


Crystal structures can be used to understand the action of drugs



The drug

Mortality rate reduced by 80% for patients where interferon did not work



Crystal structure of the drug bound to its target Abl-Kinase

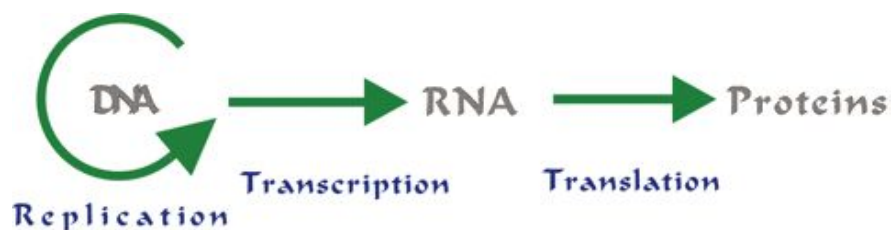
red shows resistant mutation

Thomas R. Schneider | Meth. moderner Röntgenphysik II | 25/6/2014 EMBL



The Central Dogma of Molecular Biology

- 'DNA makes RNA makes protein' (Nirenberg 2010)



<http://library.thinkquest.org/C0122429/intro/genetics.htm>

- Transcription: 'Umschreiben' of DNA (double-stranded, protected) to RNA (single-stranded, code accessible).
- Translation: Following the sequence of triplet-codons in the RNA molecule, a protein is assembled from amino acids.

Thomas R. Schneider | Meth. moderner Röntgenphysik II | 25/6/2014 EMBL



Crystal Structures support Basic Biology

- RNA Polymerase II – Structural Basis of Transcription
- 12 proteins
- ~30000 atoms
- Nobel Prize 2006 to Roger Kornberg



<http://www.youtube.com/watch?v=6QMPU9nuQso>
<http://www.lmb.uni-muenchen.de/cramer/pr-materials/index.htm>

Thomas R. Schneider | Meth. moderner Röntgenphysik II | 25/6/2014



Crystal Structures support Basic Biology

- Ribosome – Structural Basis of Translation
- 3 stretches of RNA, 52 proteins
- ~37000 RNA atoms, ~22000 protein atoms
- Nobel Price 2009 to Steitz, Yonath, Ramakrishnan



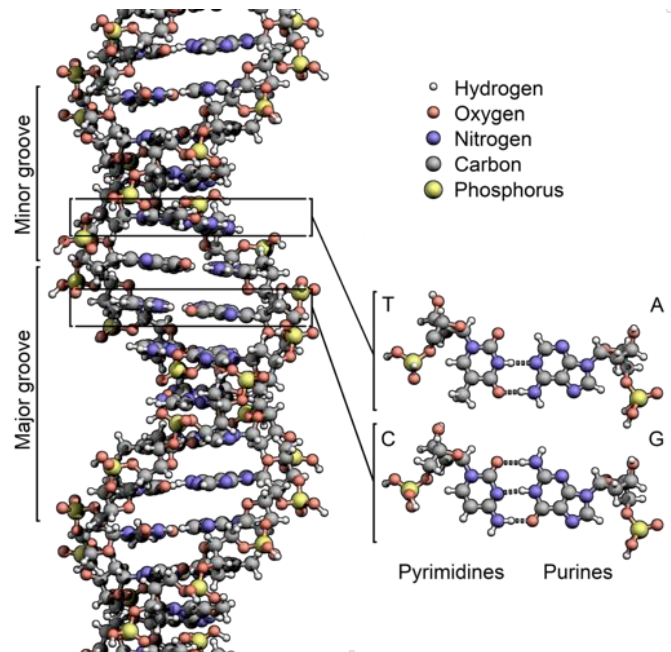
<http://www.youtube.com/watch?v=JmI8CFBWcDs>

Thomas R. Schneider | Meth. moderner Röntgenphysik II | 25/6/2014



Some milestones

DNA (1953)



Watson & Crick (1953) Nature 172:137

http://www.nobelprize.org/nobel_prizes/medicine/laureates/1962/

[http://commons.wikimedia.org/wiki/](http://commons.wikimedia.org/wiki/File:DNA_Structure%2BKey%2BLabelled.pn_NoBB.png)

[File:DNA_Structure%2BKey%2BLabelled.pn_NoBB.png](http://commons.wikimedia.org/wiki/File:DNA_Structure%2BKey%2BLabelled.pn_NoBB.png)

Myoglobin (1960)

- Started in 1954
- Structure at 2 Å resolution published in 1960
- Key-step: choose sperm-whale as source



KENDREW, J. C. et al. (1960) Nature, 185, 422–427.

http://www.nobelprize.org/nobel_prizes/chemistry/laureates/1962/kendrew-lecture.html

pdb: 1MBN



Thomas R. Schneider | Meth. moderner Röntgenphysik II | 25/6/2014 EMBL



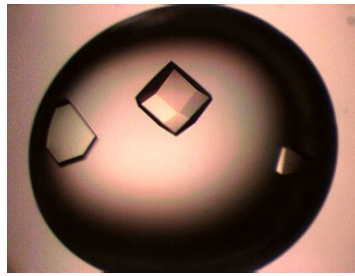
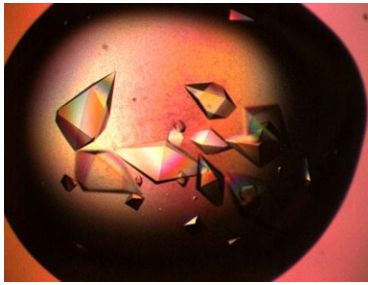
Crystals

- Are difficult to grow
- Are difficult to reproduce
- Are often very small (microns)
- Are often inhomogeneous
- Are mechanically fragile
- Are radiation sensitive

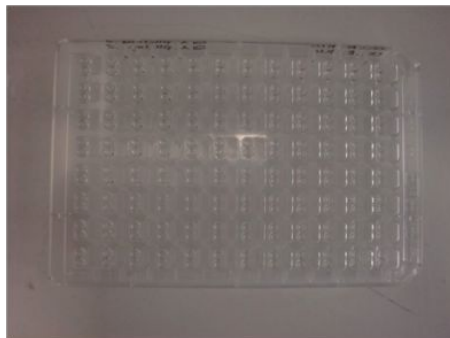
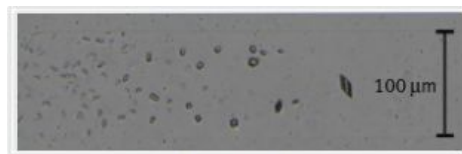
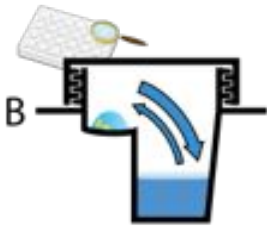
Thomas R. Schneider | Meth. moderner Röntgenphysik II | 25/6/2014 EMBL



Finding Conditions



Small Volume HTP Crystallization



96 x 50-200 nl



96 x 10 nl

High-Throughput Crystallization at EMBL Hamburg

- Miniaturization
 - 200nl/exp for vapour diffusion
 - 10nl/exp for counter diffusion
- Reference:
 - J. Müller-Dieckmann (2006) Acta Cryst. D64:1146-1152.



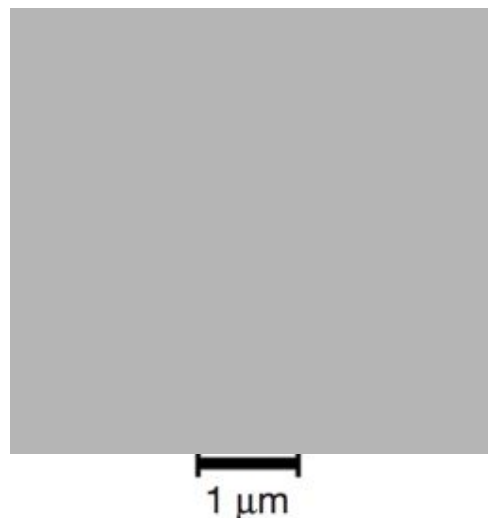
Jochen Müller-Dieckmann
Xandra Kreplin

Thomas R. Schneider | Meth. moderner Röntgenphysik II | 25/6/2014 EMBL



Small Crystals

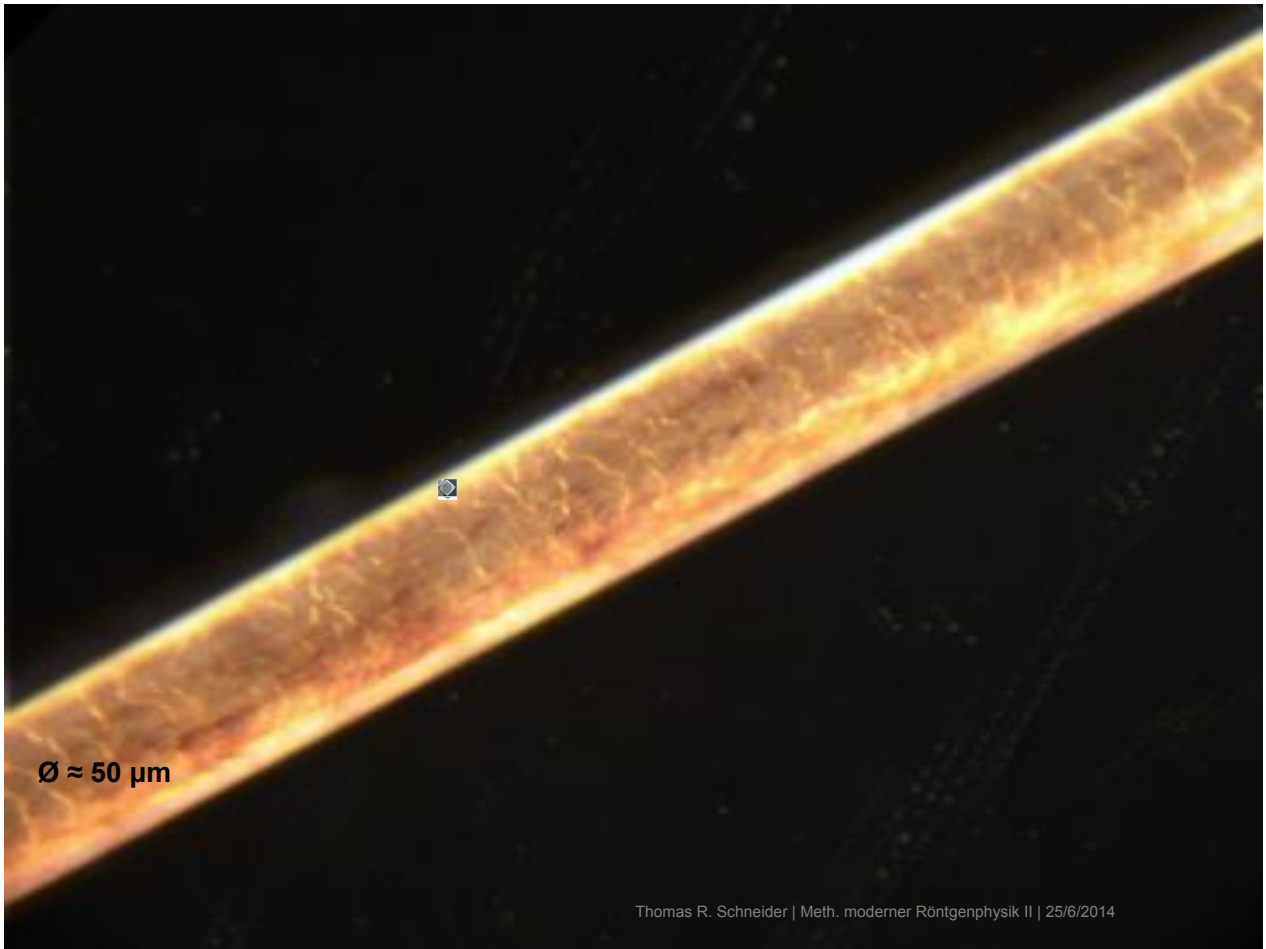
- Crystal dimensions of 1-10 micron are not rare.
- Often these crystals are of high quality
- Small and parallel beams needed.



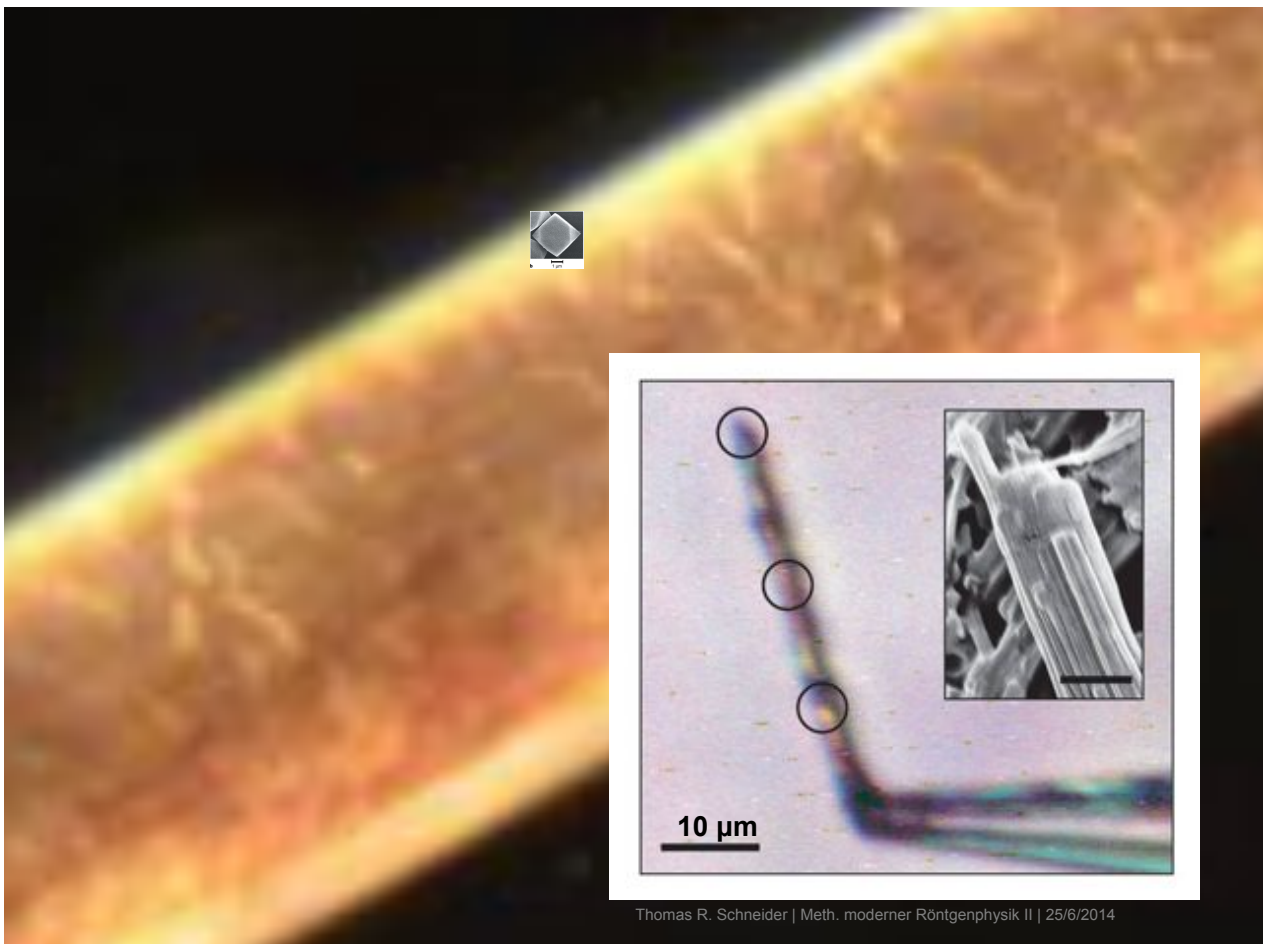
Coulibaly et al. The molecular organization of cypovirus polyhedra. Nature (2007) 446: 97-101

Thomas R. Schneider | Meth. moderner Röntgenphysik II | 25/6/2014 EMBL





Thomas R. Schneider | Meth. moderner Röntgenphysik II | 25/6/2014

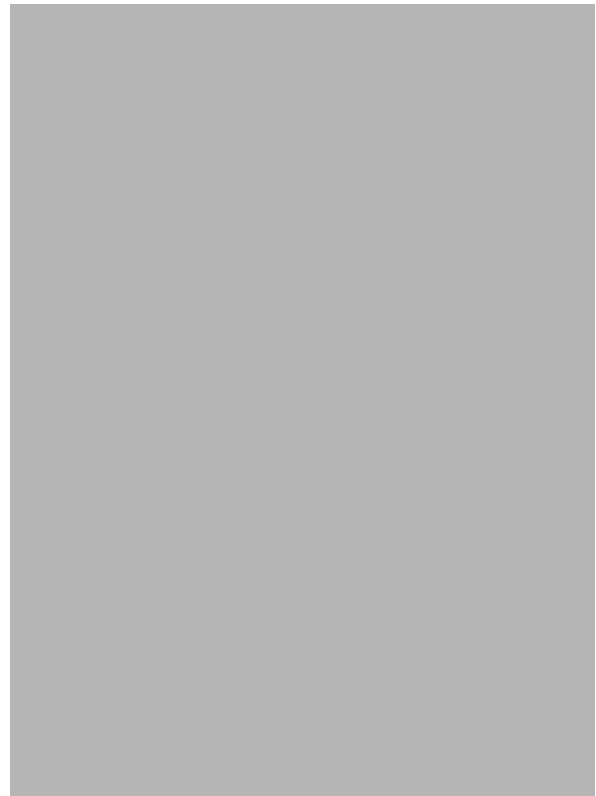


Thomas R. Schneider | Meth. moderner Röntgenphysik II | 25/6/2014

Amyloid fibrils

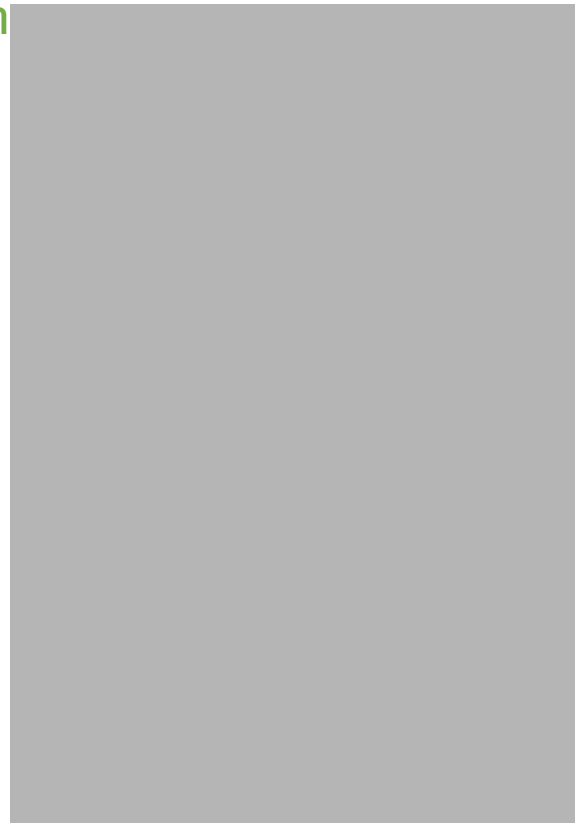


beta spine of amyloid-like fibrils.
Nature (2005) 435: 773-8



Recombinant production of proteins

- Insert DNA from other organism into bacteria (Lobban?, 1972) using enzymes as tools for the manipulation of DNA
- 1982 synthetic human insulin (Genentech & Eli Lilly) entered the market for diabetes therapy.
- Recombinant production (and 'overexpression') of protein molecules is crucial for macromolecular crystallography as large amounts of material are needed to produce crystals.



Use of synchrotron radiation in Biology

NATURE VOL. 230 APRIL 16 1971

434

NATURE VOL. 230 APRIL 16 1971

Synchrotron Radiation as a Source for X-ray Diffraction

G. ROSENBAUM & K. C. HOLMES

Max-Planck-Institut für Medizinische Forschung, Heidelberg

J. WITZ

Laboratoire des Virus des Plantes, Institut de Botanique de la Faculté des Sciences de Strasbourg, Strasbourg

Some preliminary results have been obtained with synchrotron radiation from the 7.5 GeV electron synchrotron Deutsches Elektronen-Synchrotron (DESY) in Hamburg as a source for X-ray diffraction.

When an electron is accelerated it emits radiation. At the very high energies used in DESY, the emitted radiation is confined to a narrow cone about the instantaneous direction of motion of the electron. Thus the synchrotron radiation tangentially. Synchrotron radiation is polychromatic, with a peak in the X-ray region for an electron energy of 7.5 GeV (see ref. 1 for the original theoretical description and refs. 2-4 for experimental details).

The DESY synchrotron uses bunches of 50 subbunches and each 10 ns pulse contains 4×10^{11} electrons (10 nA average beam current). The injection energy is relatively low and the electrons are accelerated up to 7.5 GeV in 10 ms.

Most of the X-radiation is emitted during the last 3 ns of each pulse; little radiation is produced at the lower electron energies, and so the time averaged intensity at 1.5 Å is about 30% of the peak value.

Table 1 Data for Quartz Monochromator in Synchrotron Radiation Beam

Synchrotron	7.5 GeV, 10 nA beam current
Electron beam	approximately 1 cm effective X-ray source diameter
Quartz	37 m from synchrotron to monochromator
Crystal of the incident beam	approximately 10^{-3} rad
Polarization	85% at 1.5 Å in the eighth arc of the cycle, polarized in the plane of the synchrotron
Re-window	0.5 mm (90 mg cm ⁻²)
Crystal	quartz cut at $45^\circ 52'$ to the 1011 plane, dimensions $45 \times 15 \times 0.5$ mm ³ (cut on face 011 mm)
Beater	layer 242 20.2 mm
Wavelength	radius of curvature of crystal, 9 m
Wavelength spread	$\Delta\lambda = 1.5 \times 10^{-4}$ Å due to deviation from lattice spacing and to finite source size
Focus	1.7 m from crystal
Angular aperture of reflected beam	horizontal: 2 mrad (vertical: 1 mrad) (vertical: 1 mrad)
Measured flux in line focus	1.1×10^{17} photons s ⁻¹ mm ⁻² of focal length (for the eighth arc of the cycle)

Table 2 Biological Applications

Specimen	Elliptic low-focus X-ray tube*	DESY synchrotron with Siemens point focusing monochromator†
Single crystal	Standard collimator 0.3 mm diameter $a = 0.5$ mm $b = 0.5$ mm $c = 1.5$ mm $J = 2 \times 10^{17}$ photons s ⁻¹ mm ⁻²	$D = 1$ m $d = 120$ μm $F = 4 \times 10^{17}$ photons s ⁻¹ mm ⁻² $f = 2.5 \times 10^{11}$ photons s ⁻¹ mm ⁻²
Tubacco mosaic virus ppt	Double-crystal focusing monochromator‡ $a = 0.6$ mm $b = 1$ mm $c = 12$ cm $J = 2 \times 10^{17}$ photons s ⁻¹ mm ⁻²	$D = 0.8$ m $d = 100$ μm $F = 3 \times 10^{17}$ photons s ⁻¹ mm ⁻² $f = 5 \times 10^{11}$ photons s ⁻¹ mm ⁻²
Insect muscle	Double-crystal focusing monochromator‡ $a = 3$ mm $b = 0.5$ mm $c = 40$ cm $J = 3 \times 10^{17}$ photons s ⁻¹ mm ⁻²	$D = 1.1$ (10 m) $d = 100$ (100 μm) $F = 5 \times 10^{17}$ (2 × 10 ¹⁷) photons s ⁻¹ mm ⁻² $f = 1.5 \times 10^{11}$ photons s ⁻¹ mm ⁻²

* a , width of specimen; b , height of specimen; c , specimen line distance; D , angle specimen distance; d , focal length; D , monochromator film diameter; d , spot or focus diameter on film; F , X-ray power reaching the specimen; and f , flux density at the focus.

† Loaded with 40 kV, 10 mA into a 0.2×2 mm² electron focus at the anode in the first case, and 40 kV, 15 mA into a 0.14×0.7 mm² focus in the other two cases. This set is the most powerful fine-focus X-ray tube currently available.

‡ The setting of the Johansson⁴ monochromator is optimized for each type of specimen.

§ Conditions of the synchrotron are as in Table 1, computed for 1.5 Å radiation. We have evaluated the spectral luminance (that is, the power in photons per second radiated per unit area, solid angle, and wavelength interval) of both the synchrotron and a fine-focus rotating anode X-ray tube (see Table 2). The values are 2×10^{17} (time averaged) and 3×10^{17} photons s⁻¹ mm⁻² Å⁻¹ respectively at 1.5 Å, showing clearly that the synchrotron is, relative to present X-ray tubes, a very bright source. The actual advantage to be gained in a diffraction experiment depends critically on the optical system necessary to focus and monochromatize the radiation. These types of focusing mono-

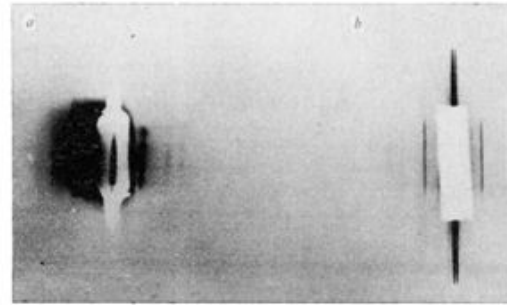


Fig. 3 Equatorial reflexions from dorsolongitudinal flight muscle of *Lethocerus maximus* recorded with: *a*, monochromated synchrotron radiation; electron energy 5 GeV, beam current 8 mA, exposure time 15 min, specimen film distance 40 cm; note the parasitic scattering on the left of the backstop arising from fluorescence from the monochromator holder; *b*, Elliott fine-focus rotating anode tube at 40 kV, 15 mA, exposure time 1 h, specimen film distance 36 cm. The strong line is the 20 reflexion ($d = 231$ Å); the weak lines are the 21, 31 and 32 reflexions.

© 1971 Nature Publishing Group

Thomas R. Schneider | Meth. moderner Röntgenphysik II | 25/6/2014

EMBL



Use of synchrotron radiation in MX

Applications of synchrotron radiation to protein crystallography: Preliminary results

(x-ray diffraction/anomalous dispersion/rubredoxin/azurin/nerve growth factor/glutaminase-asparaginase)

JAMES C. PHILLIPS, ALEXANDER WLODAWER, MARGUERITE M. YEVITZ, AND KEITH O. HODGSON*

Department of Chemistry and Stanford Synchrotron Radiation Project, Stanford University, Stanford, California 94305

Communicated by Richard H. Holm, October 23, 1975



Thomas R. Schneider | Meth. moderner Röntgenphysik II | 25/6/2014

EMBL



Detectors

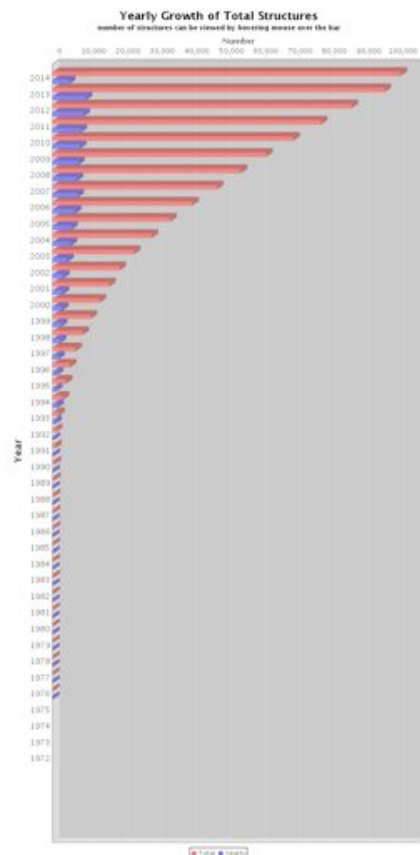
Technology	When	Readout	Remark
X-ray film	1940	30 min	grain size < 10 μm
Image Plates	1990	1.5 min	pixel: 150 x 150 μm^2 + PSF
CCD detectors	1997	1 sec	pixel: 80 x 80 μm^2 + PSF
Pixel-Array Detectors (2010)	2010	3 msec	pixel: 173 x 173 μm^2 sharp 6 MPixel
Pixel Array Detectors (2014)	2014	3 μsec	pixel: 75 x 75 μm 16 MPixel

- PSF = Point spread function



The Protein Data Bank

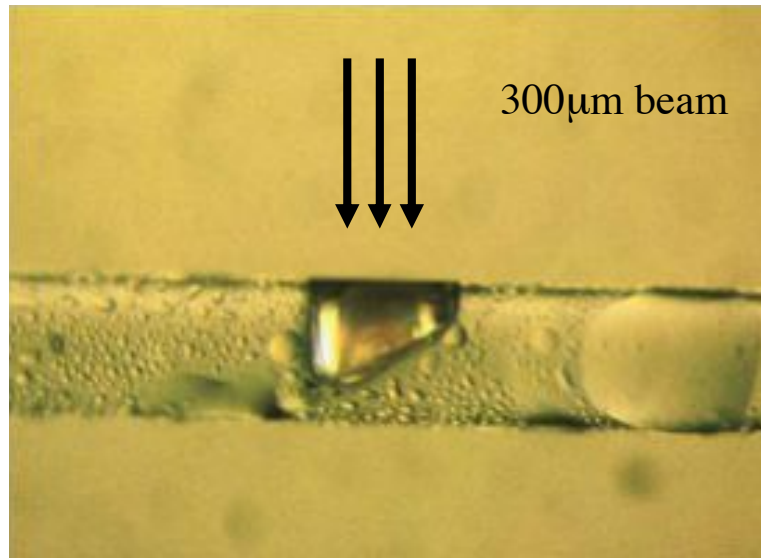
- Started as a grass-root movement in the 70's
- As of Tuesday Jun 24, 2014 17:00 PDT, **101207 structures** are in the protein data bank.
- Out of these 89670 were determined by X-ray crystallography
 - 1976:13
 - 1980:69
 - 1990: 507
 - 2000: 13596
 - 2010: 70013
 - 2014: 100000
- A large fraction of structures determined today are determined by 'Molecular Replacement'



<http://www.rcsb.org/pdb/statistics/contentGrowthChart.do?content=total&seqid=100>



Radiation Damage



Garman & Schneider (1997) J. Appl. Cryst. 30:211

Thomas R. Schneider | Meth. moderner Röntgenphysik II | 25/6/2014



Data collection at 100 K

- Mounting protein-crystals in a free-standing film revolutionized the field.

Teng, T. Y. (1990)
J. Appl. Cryst 23: 387-391

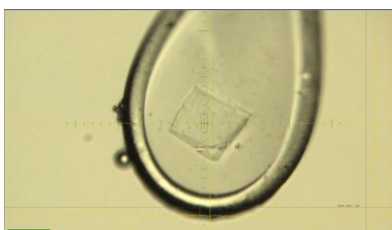
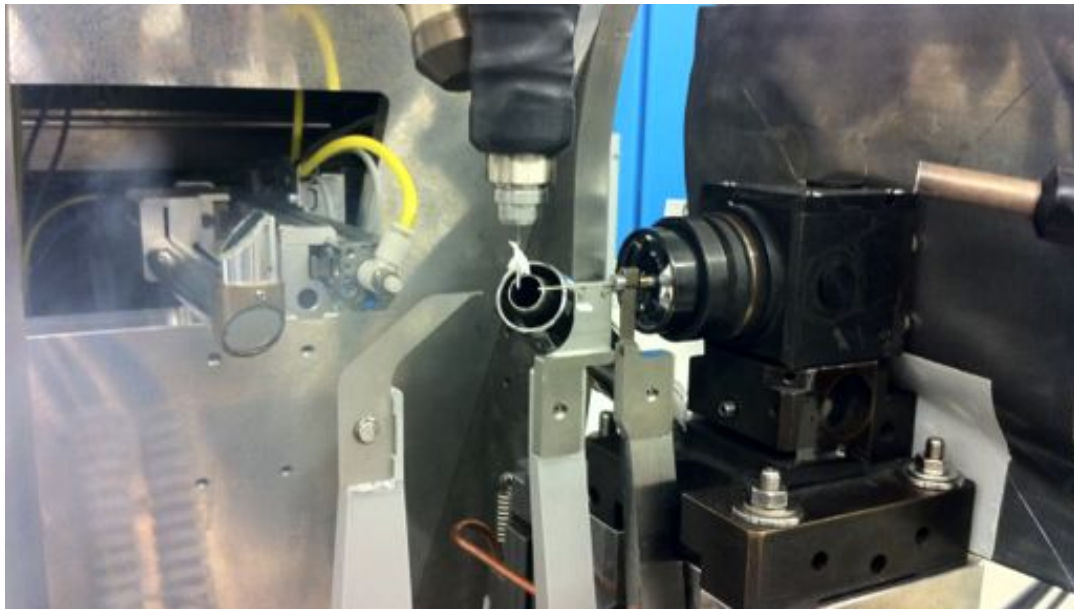


Fig. 2. The loop mounted on an oscillation camera used at CHESS: *A* cold nitrogen nozzle; *B* the loop with a frozen crystal; *C* cold-gas-stream reflector mounted on the goniometer head. The cold nitrogen nozzle (*A*) of a transfer line is 1/4 in diameter which delivers a gas stream at from 80 to 230 K. Within a cone-shaped working volume of 65 mm³, the temperature gradient is less than 4 K, at an initial exit temperature of 85 K. Fog or ice formation around the nozzle, crystal and goniometer head is avoided by a coaxial warm and dry nitrogen stream that surrounds the cold stream, and by a built-in heater on the base of the cold-gas-stream reflector (*C*).

Thomas R. Schneider | Meth. moderner Röntgenphysik II | 25/6/2014



HPGonioV: Sample environment

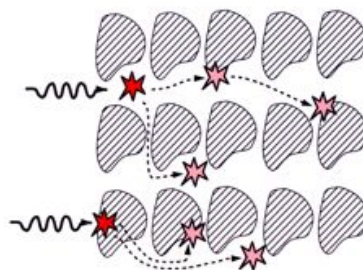
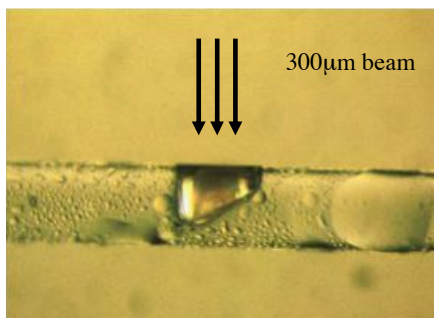
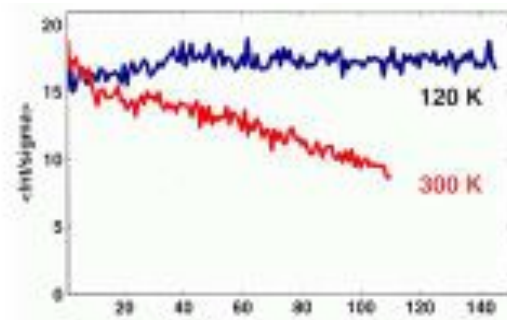


- 400 micron thick blade.
- Motorized adjustable distance to sample: 7-36 mm.

Thomas R. Schneider | Meth. moderner Röntgenphysik II | 25/6/2014 EMBL 

Radiation Damage

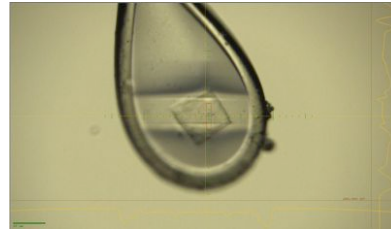
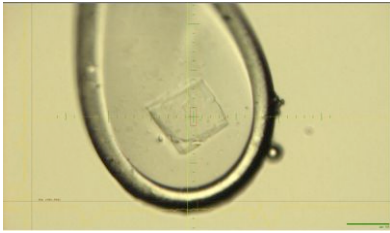
- Data collection at 100 K significantly extends crystal lifetime (factor of 50)



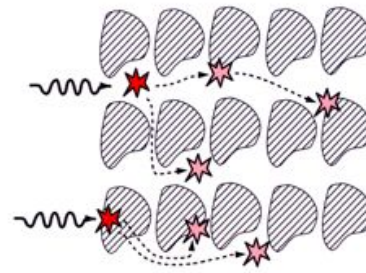
Garman & Schneider (1997) J. Appl. Cryst. 30:211

Thomas R. Schneider | Meth. moderner Röntgenphysik II | 25/6/2014 EMBL 

Radiation damage at 100 K

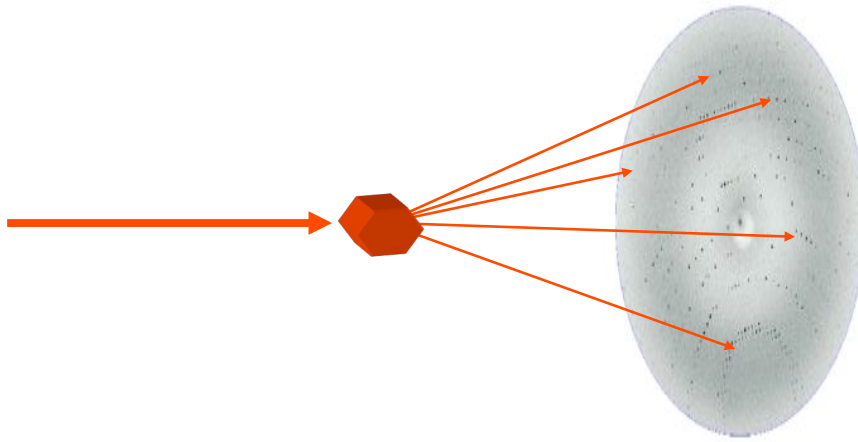


- On modern synchrotron beamlines the lifetime of protein crystals at 100k is on the order of seconds to minutes.
- Going back to Room temperature, Owen et al. (2012) Acta Cryst. D68:810 have shown that in the first 200 msec of a room temperature experiment, one can outrun hydroxyl radicals.



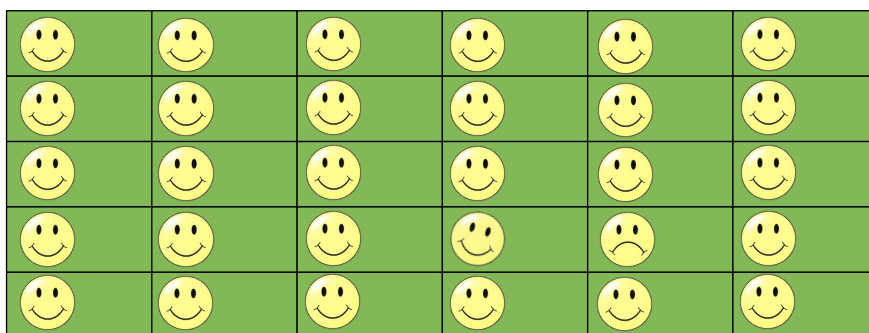
Crystal Structure Determination

Diffraction from a Crystal



Thomas R. Schneider | Meth. moderner Röntgenphysik II | 25/6/2014 EMBL 

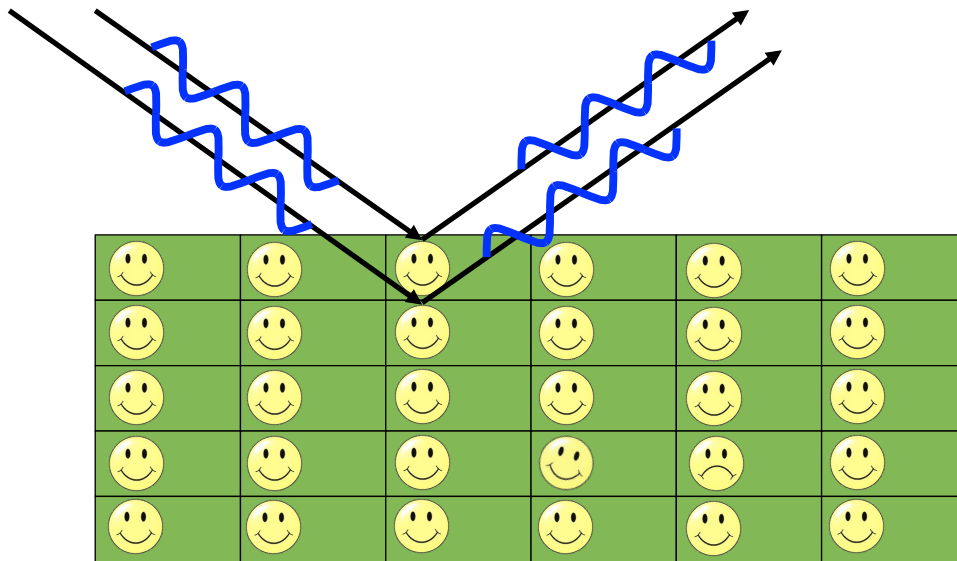
Inside a crystal



- A crystal consists of repeating units, the crystallographic unit cells.
- Each unit cells has 'the same' content, i.e. the same molecules in the same conformation and in the same orientation
- In real crystals, there is always some amount of 'disorder'

Thomas R. Schneider | Meth. moderner Röntgenphysik II | 25/6/2014 EMBL 

Diffraction from a crystal

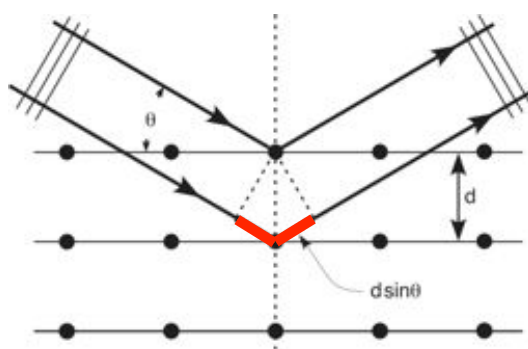


- When electromagnetic waves are interacting with a periodic structure, interference effects will occur.

Thomas R. Schneider | Meth. moderner Röntgenphysik II | 25/6/2014 EMBL 

Diffraction planes

http://en.wikipedia.org/wiki/X-ray_crystallography



Constructive interference occurs when Bragg's law is fulfilled:

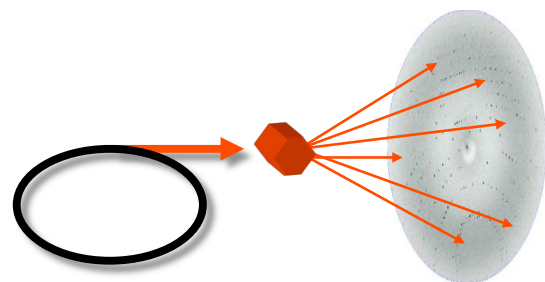
$$2 d \sin\theta = n \lambda$$



Nobel prize for physics 1914 to Max von Laue



Nobel prize for physics 1915 to William and Lawrence Bragg

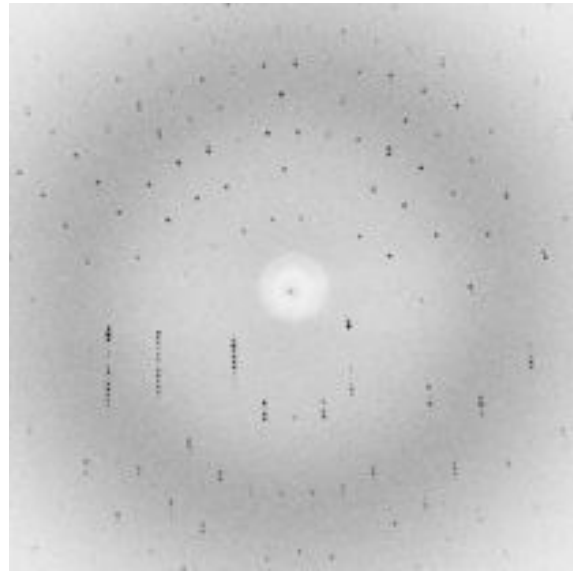


IYCr2013

Thomas R. Schneider | Meth. moderner Röntgenphysik II | 25/6/2014 EMBL 

Diffraction Data

- The diffraction pattern changes when the crystal is rotated.
- By rotating the crystal, different Bragg-planes are brought into their diffracting position



http://www-structmed.cimr.cam.ac.uk/Course/Basic_diffraction/data_animation.html

Thomas R. Schneider | Meth. moderner Röntgenphysik II | 25/6/2014 EMBL



Diffraction and forests ...



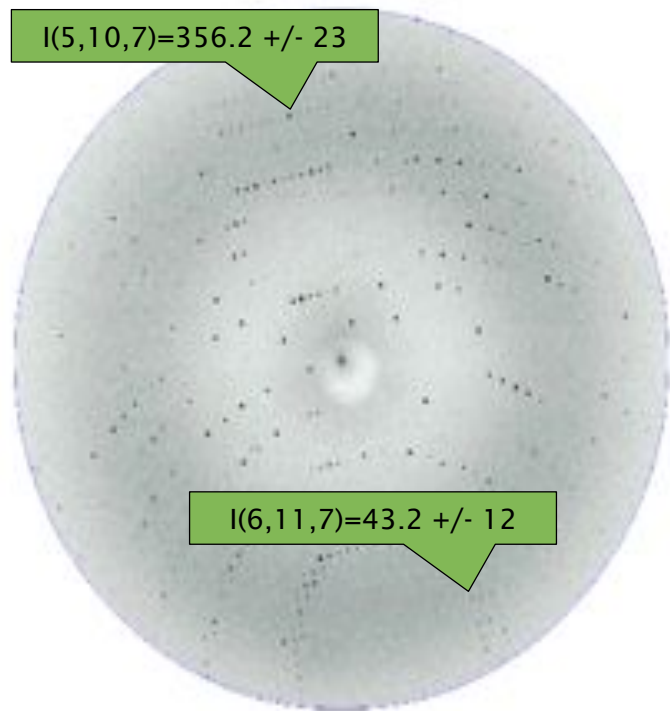
<http://flickr.com/photos/rossogiallobianco/2486114038>

Thomas R. Schneider | Meth. moderner Röntgenphysik II | 25/6/2014 EMBL



Indices and Structure factor amplitudes

- Every diffraction spot is marked by an index hkl
- For every diffraction spot an Intensity I is measured.
- The result of the experiment is an indexed set of I's
- Diffraction at low 2theta is stronger than at high 2theta



Diffraction data

h	k	l	I	sig(I)
0	20	35	4980.5	122.6
0	20	36	6906.6	216.6
0	20	37	8302.3	231.7
0	20	38	3209.5	89.3
0	20	39	459.6	22.1
0	20	40	1017.4	33.8
0	20	41	-5.6	18.3
0	20	42	33.8	15.6
0	20	43	4545.7	133.4
0	20	44	210.5	19.2
0	20	45	808.8	29.1



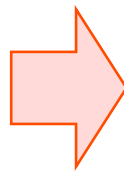
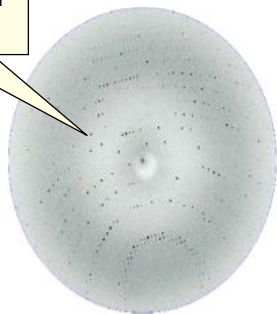
Structure Factor Amplitudes

- For formal reasons, the measured I's are usually converted to 'Structure Factor Amplitudes' F by:

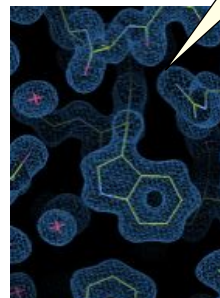
$$F = \sqrt{I}$$

Calculating Electron density

Intensity I_{hkl} for some set of planes with Miller indices hkl



Electron density for all points in the unit cell



$$\rho_{xyz} = \sum_{hkl} |F_{hkl}| e^{-i\varphi_{hkl}} e^{-2\pi i(hx+ky+lz)}$$

Electron density at some point xyz in space

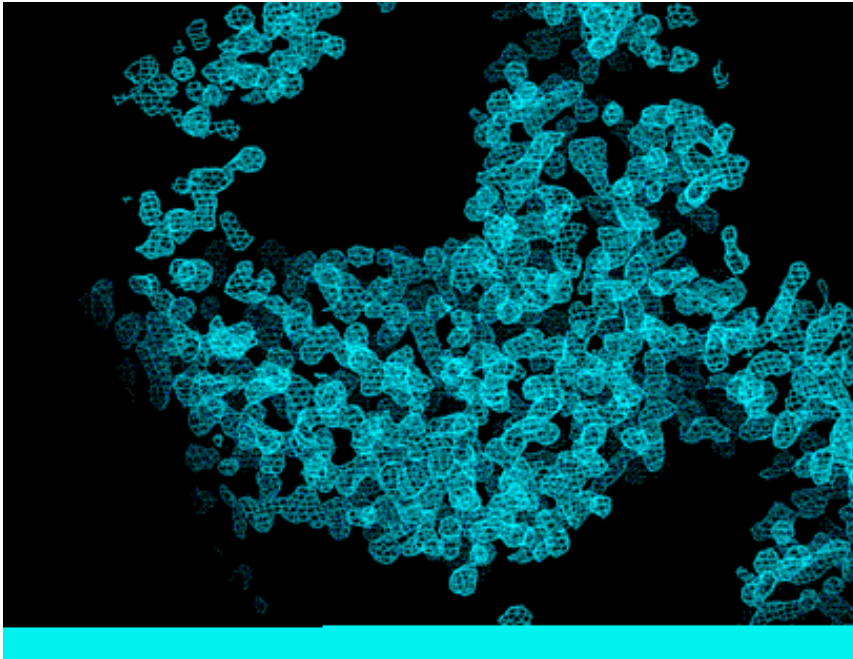
Sum over all Bragg reflections

Structure Factor Amplitude for each reflection hkl. $F_{hkl} \approx \sqrt{I_{hkl}}$

Structure Factor Phase for each reflection hkl.

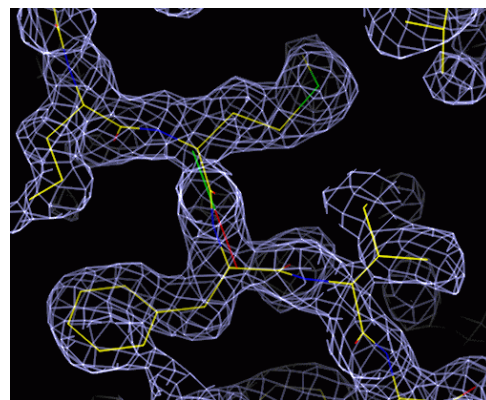
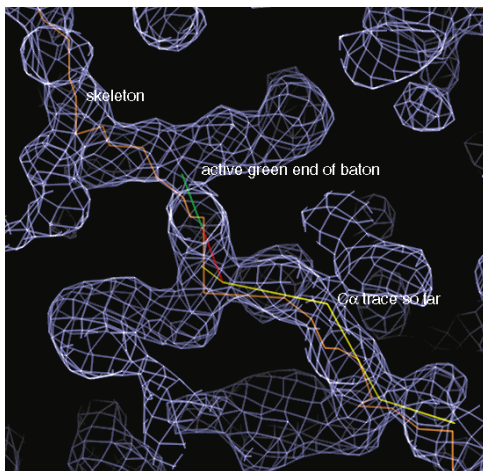
Phase shift depending on hkl and position in space

Typical initial electron density map



Thomas R. Schneider | Meth. moderner Röntgenphysik II | 25/6/2014 EMBL 

Interpretation of the electron density map



Thomas R. Schneider | Meth. moderner Röntgenphysik II | 25/6/2014 EMBL 

A 'pdb'-file (www.rcsb.org)

```
HEADER      TRANSFERASE                               06-MAR-03  1OPJ
TITLE      STRUCTURAL BASIS FOR THE AUTO-INHIBITION OF C-ABL TYROSINE
TITLE      2 KINASE
.
.
ATOM       1  N  ALA A 243      20.064 -2.529 43.315  1.00 51.64      N
ATOM       2  CA ALA A 243      19.658 -1.370 42.459  1.00 51.36      C
ATOM       3  C  ALA A 243      20.832 -0.838 41.643  1.00 50.91      C
ATOM       4  O  ALA A 243      20.650  0.010 40.776  1.00 50.77      O
ATOM       5  CB ALA A 243      19.092 -0.263 43.322  1.00 50.20      C
ATOM       6  N  MET A 244      22.030 -1.350 41.906  1.00 50.62      N
ATOM       7  CA MET A 244      23.218 -0.888 41.195  1.00 50.73      C
ATOM       8  C  MET A 244      23.537 -1.709 39.950  1.00 50.43      C
ATOM       9  O  MET A 244      24.554 -1.488 39.298  1.00 50.33      O
ATOM      10  CB MET A 244      24.420 -0.882 42.146  1.00 51.32      C
ATOM      11  CG MET A 244      24.215  0.020 43.361  1.00 52.32      C
ATOM      12  SD MET A 244      25.597  0.070 44.515  1.00 54.49      S
ATOM      13  CE MET A 244      26.730  1.130 43.627  1.00 53.37      C
ATOM      14  N  ASP A 245      22.662 -2.653 39.620  1.00 49.87      N
ATOM      15  CA ASP A 245      22.857 -3.505 38.446  1.00 49.28      C
ATOM      16  C  ASP A 245      22.115 -2.895 37.257  1.00 47.55      C
```